Physical Review B 94. 174106 Supplemental Material (2016),

Pressure-induced phase transitions in the $CdCr_2Se_4$ spinel

I. Efthimiopoulos[1,2], Z. T. Y. Liu[3], M. Kucway[1], S. V. Khare[3], P. Sarin[4], V. Tsurkan[5,6], A. Loidl[6], and Y. Wang[1,‡]

[1]*Department of Physics, Oakland University, Rochester, Michigan 48309, USA*

[2]*Deutsches GeoForschungsZentrum GFZ, Section 4.3, Telegrafenberg, 14473, Potsdam, Germany*

[3]*Department of Physics, University of Toledo, Toledo, Ohio 43606, USA*

[4]*School of Materials Science and Engineering, Oklahoma State University, Tulsa, Oklahoma 74106, USA*

[5]*Institute of Applied Physics, Academy of Sciences of Moldova, MD-2028 Chisinau, Republic of Moldova*

[6]*Experimental Physics 5, Center for Electronic Correlations and Magnetism, Institute of Physics, University of Augsburg, D-86159 Augsburg, Germany*

SUPPLEMENTARY INFORMATION

Table S1: Experimentally determined structural parameters for the $Fd\bar{3}m$ (Z = 8), the $I4_1/amd$ (Z = 4), and the orthorhombic (Z = 4) phases of $CdCr_2Se_4$.

$Fd\bar{3}m$ [a]	P (GPa)	a (Å)	V (Å^3)	Se-u	Cd-Se (Å)	Cr-Se (Å)	Cr-Se-Cr (^{o})
	1 bar	10.74645(1)	1241.07	0.2647(1)	2.60	2.54	96.90
	1.4	10.69154(1)	1222.14	0.2643(1)	2.58	2.53	96.70
	2.7	10.63793(1)	1203.84	0.2637(1)	2.56	2.52	96.40
	3.9	10.59759(1)	1190.21	0.2646(1)	2.56	2.50	96.84
	5.1	10.55519(1)	1175.97	0.2644(1)	2.55	2.50	96.76
	6	10.52646(1)	1166.40	0.2636(1)	2.53	2.50	96.35
	7.5	10.47808(1)	1150.39	0.2633(1)	2.51	2.49	96.24
	8.6	10.4454(1)	1139.66	0.2632(1)	2.50	2.48	96.18
	9.2	10.4316(1)	1135.16	0.2625(1)	2.48	2.48	95.83
	11.6	10.3739(1)	1116.42				
$I4_1/amd$ [b]		**a (Å)**	**c (Å)**	**c/a***	**V (Å^3)**	**Se-y**	**Se-z**
	11.6	7.8198(1)	8.7600(1)	0.792	535.7		
	12.9	7.8158(1)	8.6463(1)	0.782	528.2	0.0593(1)	0.2658(2)
	14	7.8140(1)	8.4782(1)	0.767	517.7	0.0621(2)	0.2745(3)
Orthorhombic		**a (Å)**	**b (Å)**	**c (Å)**	**c/a***	**b/a**	**V (Å^3)**
	15.4	7.732(2)	7.846(1)	8.421(1)	0.770	1.015	510.9
	16.2	7.717(2)	7.818(1)	8.392(1)	0.769	1.013	506.3
	19	7.669(2)	7.788(1)	8.293(1)	0.765	1.016	495.4
	21.3	7.634(2)	7.756(1)	8.223(1)	0.762	1.016	486.9
	23.2	7.587(2)	7.731(1)	8.176(1)	0.762	1.019	479.6
	25.2	7.579(2)	7.695(1)	8.146(1)	0.760	1.015	475.2
	27.6	7.490(2)	7.648(1)	8.067(1)	0.762	1.021	462.1

[a] **Wyckoff positions:** Cd (8a: 0.125, 0.125, 0.125), Cr (16d: 0.5, 0.5, 0.5), Se (32e: u, u, u)

Isotropic atomic displacement parameters U_{iso}: $U_{iso,Cd}$ = 0.003(1) Å^2, $U_{iso,Cr}$ = 0.007(2) Å^2, $U_{iso,Se}$ = 0.005(3) Å^2

[b] **Wyckoff positions:** Cd (4a: 0, 0.75, 0.125), Cr (8d: 0, 0, 0.5), Se (16h: 0, y, z)

U_{iso}: $U_{iso,Cd}$ = 0.003 Å^2 (fixed), $U_{iso,Cr}$ = 0.007 Å^2 (fixed), $U_{iso,Se}$ = 0.005 Å^2 (fixed)

Table S1: DFT calculated cell parameters of the $Fd\bar{3}m$ (Z = 8) $CdCr_2Se_4$ phase with respect to pressure.

P **(GPa)**	***V*** **(Å^3)**	***a*** **(Å)**	***E*** **(eV)**
-2.7	1342.236	11.03087	-75.2
-0.7	1301.358	10.91773	-75.3
1.6	1256.373	10.79045	-75.3
4.5	1212.437	10.66317	-75.1
7.9	1169.537	10.53589	-74.7
12.1	1123.07	10.39447	-74.0
17.1	1077.852	10.25305	-73.0

Table S2: DFT calculated cell parameters of the tetragonal AFM1 phase with respect to pressure. Notice that beyond 15 GPa there is large inequality of the *a* and *b* axes, and the cell is essentially orthorhombic.

P **(GPa)**	***V*** **(Å^3)**	***a*** **(Å)**	***b*** **(Å)**	***c*** **(Å)**	***E*** **(eV)**
0.1	670.0	7.82	7.83	10.93	-149.9
1.5	641.3	7.71	7.71	10.78	-150.1
3.4	612.5	7.60	7.61	10.60	-149.8
5.8	583.7	7.49	7.50	10.39	-148.9
8.8	555.0	7.75	7.74	9.25	-147.1
12.7	526.2	7.83	7.81	8.61	-145.3
17.8	497.5	7.70	7.77	8.32	-142.8
24.5	468.7	7.46	7.73	8.13	-139.1
33.4	440.0	7.24	7.67	7.93	-134.0

Table S3: DFT calculated cell parameters of the tetragonal AFM2 phase with respect to pressure. Notice that beyond 15 GPa there is large inequality of the *a* and *b* axes, and the cell is essentially orthorhombic.

P **(GPa)**	***V*** **(Å^3)**	***a*** **(Å)**	***b*** **(Å)**	***c*** **(Å)**	***E*** **(eV)**
-0.9	672.0	7.85	7.81	10.96	-150.1
1.2	640.0	7.71	7.66	10.84	-150.4
3.7	608.0	7.58	7.52	10.66	-150.0
6.9	576.0	7.46	7.41	10.42	-148.7
10.8	544.0	7.84	7.85	8.84	-146.7
15.8	512.0	7.78	7.79	8.44	-144.2
22.2	480.0	7.59	7.75	8.16	-140.6
27.0	460.0	7.41	7.71	8.04	-137.6
32.7	440.0	7.25	7.67	7.92	-133.8

Table S5: Atomic positions of the tetragonal phase of $CdCr_2Se_4$. This cell is a prototype transformed from the conventional cubic unit cell of the spinel structure at 0 GPa. Relaxations were done to ensure optimized cell shape and atomic positions.

Lattice vectors (Å)	**x**	**y**	**z**
a	7.688	0.000	0.000
b	0.000	7.688	0.000
c	0.000	0.000	8.873

Atom	**Relative coordinates**			**Atom**	**Relative coordinates**		
	$\mathbf{u_1}$	$\mathbf{u_2}$	$\mathbf{u_3}$		$\mathbf{u_1}$	$\mathbf{u_2}$	$\mathbf{u_3}$
Cd	0.000	0.500	0.250	Se	0.781	0.500	0.641
Cd	0.500	0.000	0.750	Se	0.719	0.000	0.141
Cd	0.500	0.500	0.500	Se	0.500	0.281	0.891
Cd	0.000	0.000	0.000	Se	0.000	0.219	0.391
Cr	0.750	0.500	0.875	Se	0.719	0.500	0.109
Cr	0.750	0.000	0.375	Se	0.781	0.000	0.609
Cr	0.500	0.250	0.125	Se	0.000	0.281	0.859
Cr	0.000	0.250	0.625	Se	0.500	0.219	0.359
Cr	0.250	0.000	0.375	Se	0.219	0.000	0.609
Cr	0.250	0.500	0.875	Se	0.281	0.500	0.109
Cr	0.000	0.750	0.625	Se	0.281	0.000	0.141
Cr	0.500	0.750	0.125	Se	0.219	0.500	0.641
				Se	0.000	0.781	0.391
				Se	0.500	0.719	0.891
				Se	0.500	0.781	0.359
				Se	0.000	0.719	0.859

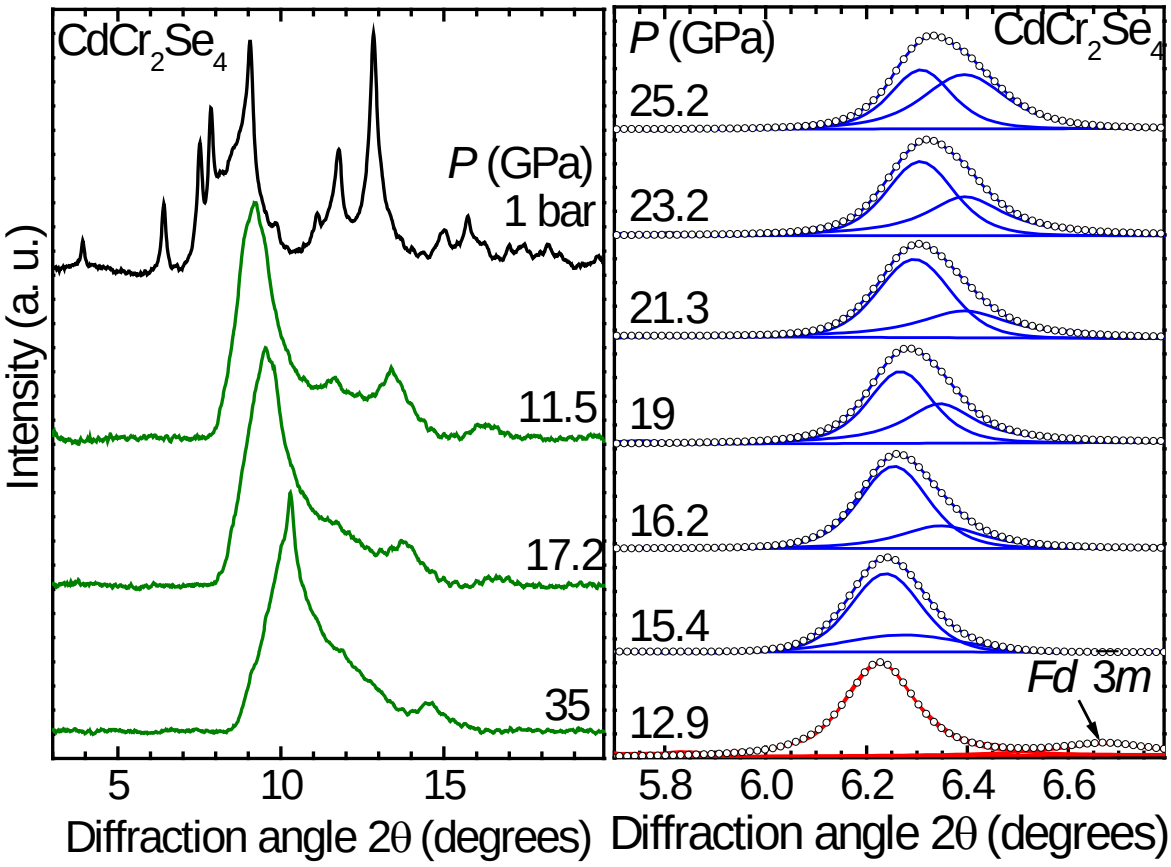

FIG. S1: (Left) XRD patterns of $CdCr_2Se_4$ collected during decompression (T = 300 K, λ = 0.4246 Å). The black and blue spectra correspond to the $Fd\bar{3}m$ and the disordered phase, respectively. Background has been subtracted for clarity. (Right) Enhanced view of the $I4_1/amd$ (200) Bragg peak in the vicinity of the tetragonal-orthorhombic transition. The orthrohombic distortion is recognized by the splitting of this peak into two components at 15.4 GPa.

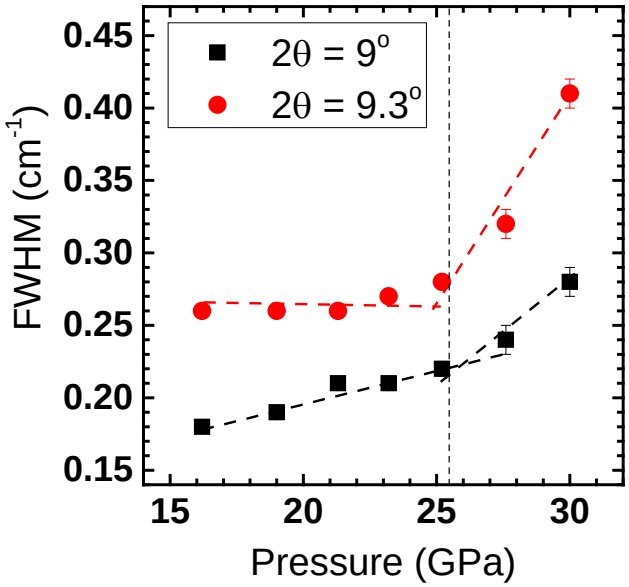

FIG S2: Evolution of the Bragg peak widths for two peaks of the orthorhombic phase. Notice the increase above 25 GPa, indicating the onset of structural disorder.

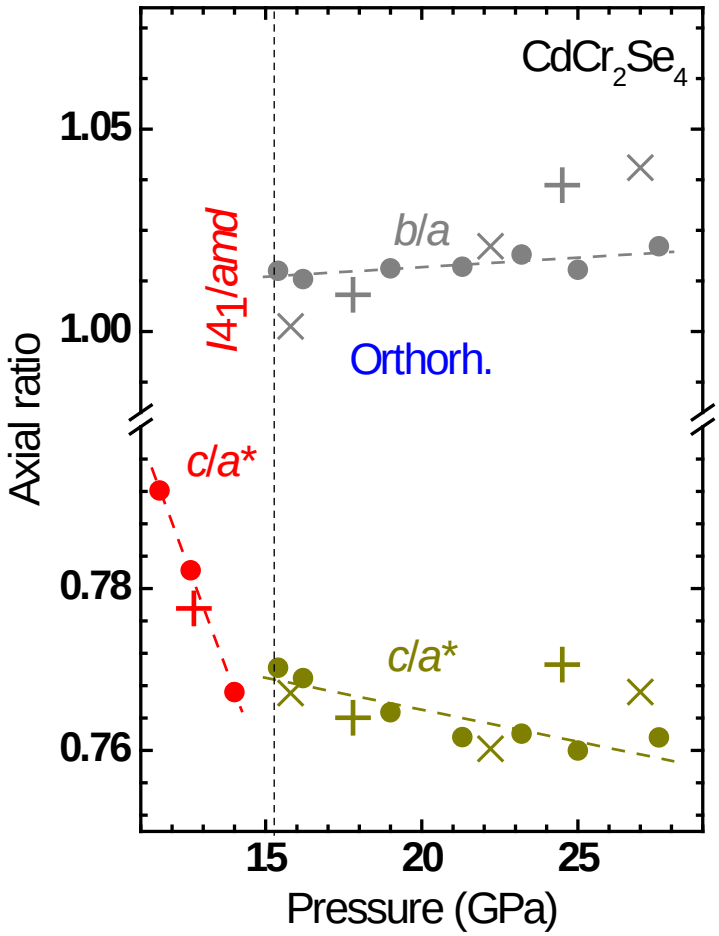

FIG. S3: Lattice parameter ratios as a function of pressure for the high-pressure tetragonal and orthorhombic phases of $CdCr_2Se_4$ (error bars lie within the symbols). The closed and open symbols correspond to experimental and DFT data, respectively (+: AFM1, ×: AFM2, $a^* = \sqrt{2}a$). The dashed lines through the symbols serve as guides to the eye, whereas the vertical dashed line mark the tetragonal-orthorhombic structural transition.

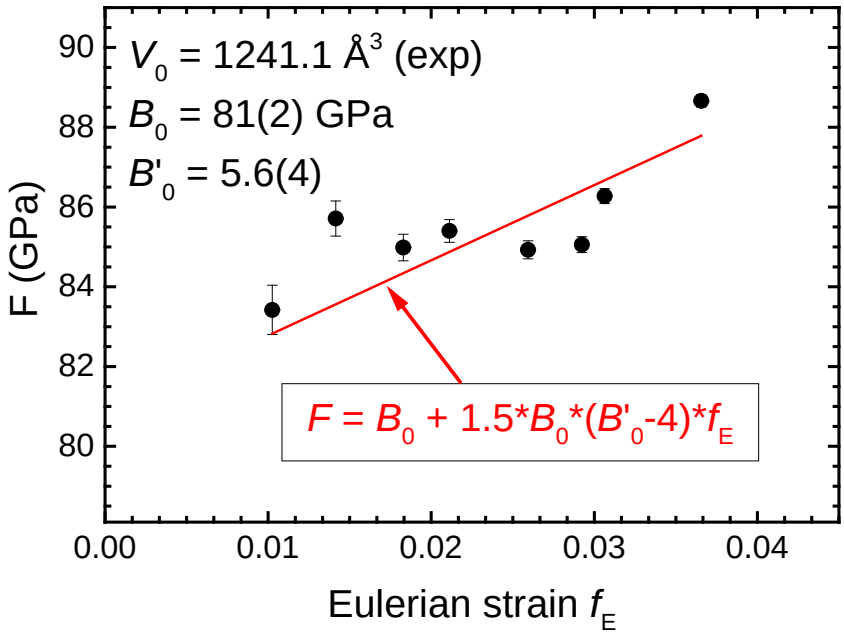

FIG S4: Plot of the normalized stress F as a function of the Eulerian strain f_E for the $Fd\bar{3}m$ phase of $CdCr_2S_4$. The F-f_E quantities are calculated from the P-V data (**Table S1**) as follows: $f_E = [(V_0/V)^{2/3}-1]/2$ and $F = P/3f_E(1+2f_E)^{5/2}$, where V_0 is the ambient-pressure volume, V is volume, and P stands for pressure[1]. Since V_0 is not known for the $I4_1/amd$ and orthorhombic phases, we did not apply this procedure for both of these high-pressure modifications.

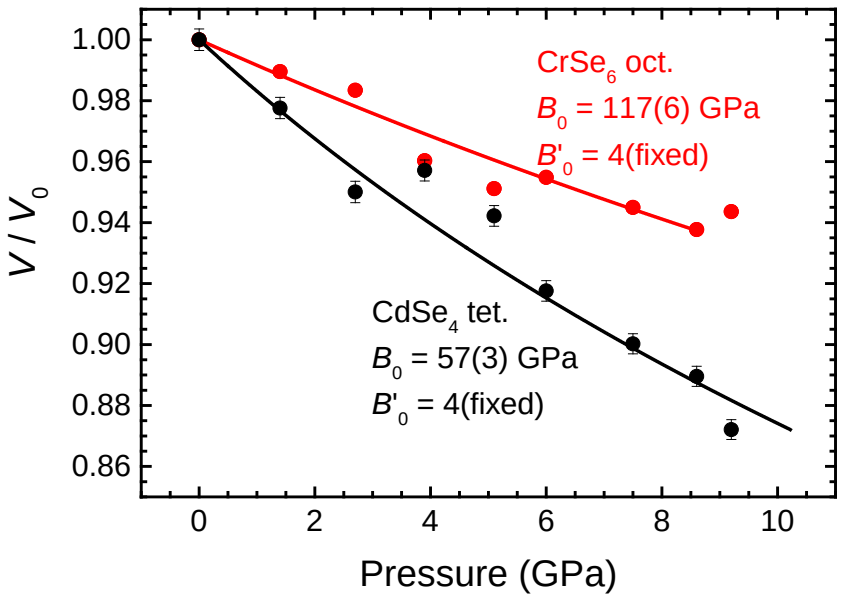

FIG. S5: Pressure-induced variation of the normalized polyhedral volume for the $Fd\bar{3}m$ phase of $CdCr_2S_4$. The black and red circles correspond to the $CdSe_4$ tetrahedral and the $CrSe_6$ octahedral volumes, respectively. The solid lines are fitted second-order Birch-Murnaghan equations of state[2,3].

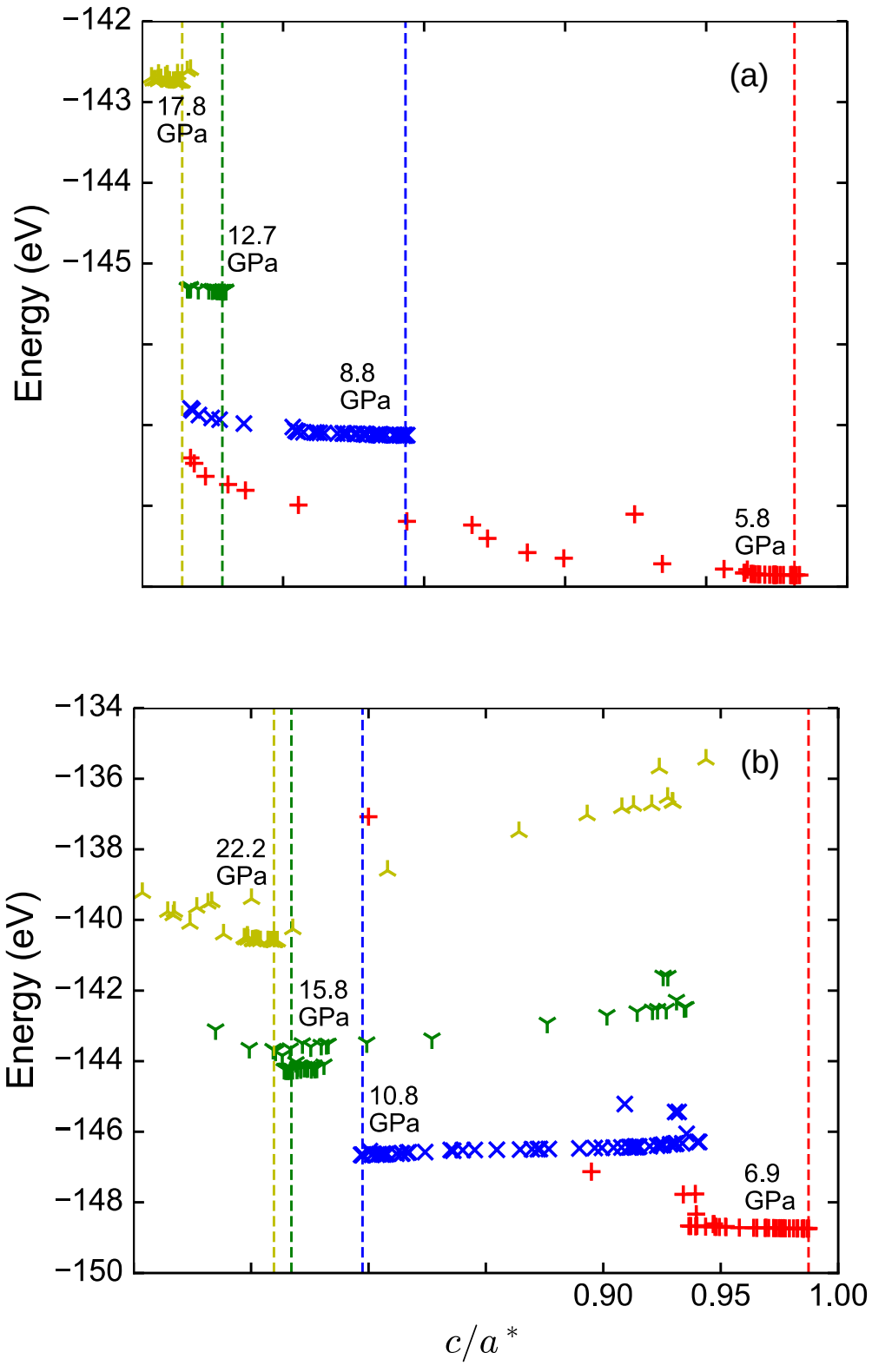

FIG S6: Relaxation traces of the c/a^* ratios at different pressure points for (a) AFM1 and (b) AFM2 phases. For each pressure, the energy is lowered as the structure reaches the final c/a^* ratio ($a^* = \sqrt{2}a$).

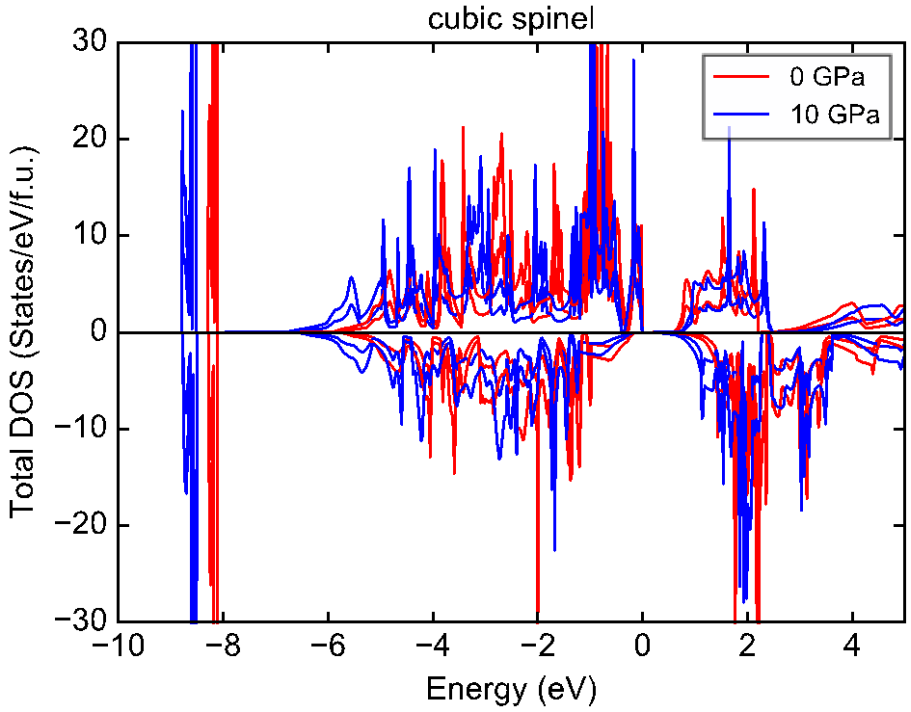
cubic spinel
0 GPa
10 GPa
Total DOS (States/eV/f.u.)
Energy (eV)
30
20
10
0
−10
−20
−30
−10
−8
−6
−4
−2
0
2
4

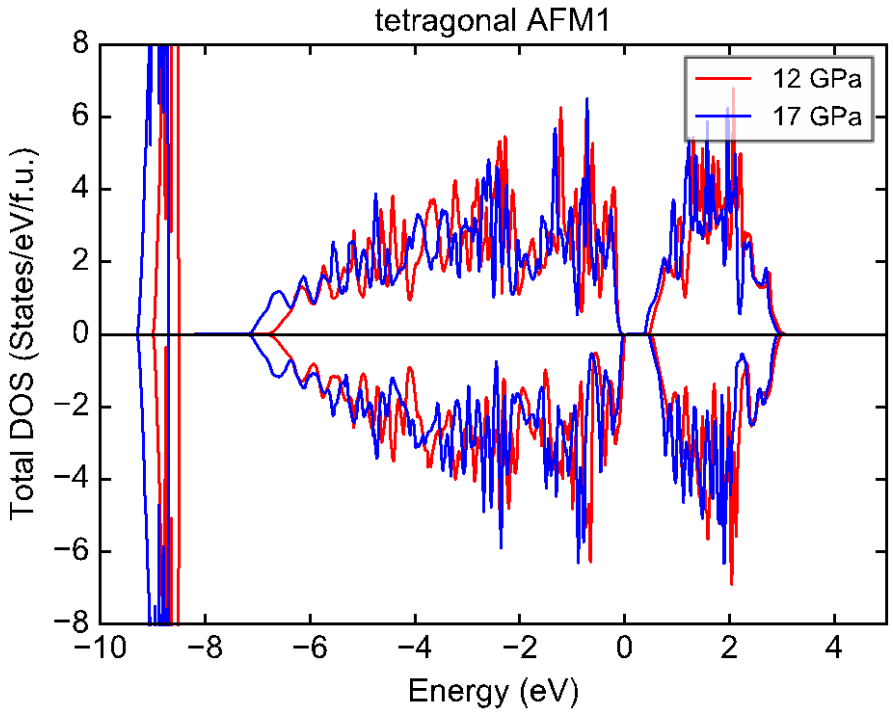
tetragonal AFM1
12 GPa
17 GPa
Total DOS (States/eV/f.u.)
Energy (eV)
8
6
4
2
0
−2
−4
−6
−8
−10
−8
−6
−4
−2
0
2
4

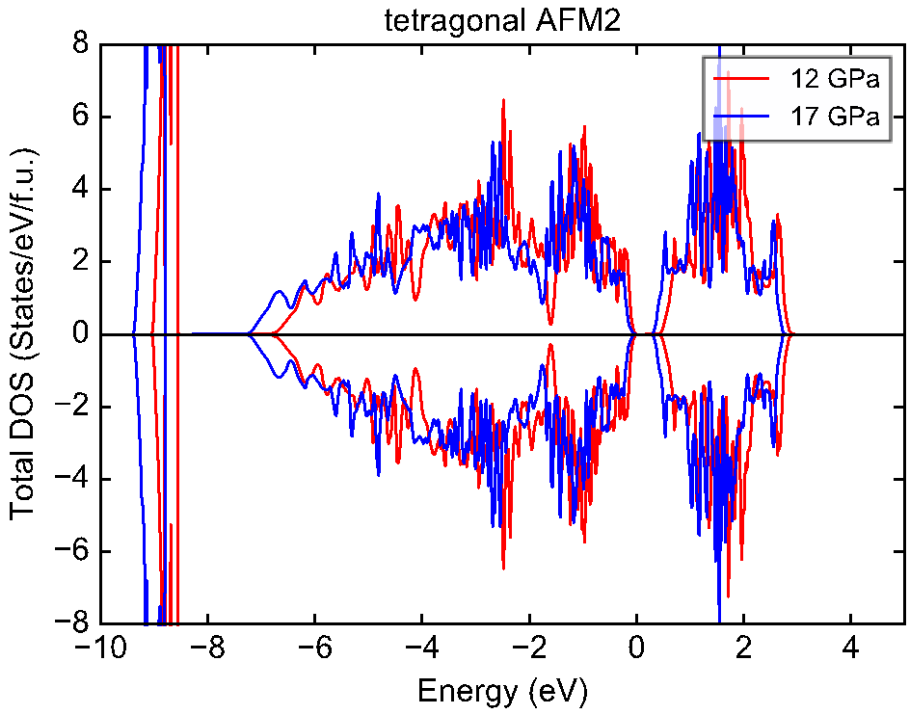

FIG S7: Electronic total denstity of states (DOS) per formula unit (f.u.) of the cubic and the high-pressure tetragonal AFM1 and AFM2 phases at various pressures. Spin-up states are above *x*-axis, whereas the spin-down states lie below. Note that the calculations were performed with regular PBE potentials rather than HSE06.

REFERENCES

[1] R.J. Angel, Rev. Miner. Geochem. **41**, 35 (2000).

[2] F. Birch, Phys. Rev. **71**, 809 (1947).

[3] F. Birch, J. Geophys. Res. **83**, 1257 (1978).